MJFAS MALAYSIAN JOURNAL OF FUNDAMENTAL AND APPLIED SCIENCES
PRINT ISSN: 2289-5981 | ONLINE ISSN: 2289-599X

RESEARCH ARTICLE

# Comparison between incident and reflected of two modes waves correlation with various porosities and thicknesses of bone phantom

Muhamad Amin Abd Wahab*, Rubita Sudirman, Mohd Azhar Abdul Razak, Nasrul Humaimi Mahmood

[a] School of Electrical Engineering, Faculty of Engineering, Universiti Teknologi Malaysia, UTM Johor Bahru, 81310 Johor, Malaysia.

* Corresponding author: mamin55@liveutm.onmicrosoft.com

**Article history**
Received 22 April 2020
Revised 30 May 2020
Accepted 5 July 2020
Published Online 20 October 2020

**Abstract**

The accuracy of the ultrasound measurement using through transmission technique to estimate bone quality based on fast and slow wave analysis is getting better but limited to the certain part of the skeletal site. Thus, the pulse echo technique with the application of fast and slow wave analysis is proposed to solve the problem as the technique only uses one transducer to operate. The objective of this paper is to conduct experiments using through transmission and pulse echo technique to study the relationship of fast and slow wave with various porosity of three different thicknesses of polyurethane foam. Fast and slow waves will be separated from the "incident" and "reflected" wave (mix wave) by utilizing bandlimited deconvolution method. Then, the ultrasound parameters for mix, fast and slow waves for both incident and reflection waves are computed, plotted against porosity for each thickness and the results is compared in terms of the correlation coefficient. The overall results show that, the slope of attenuation of the incident fast waves shows a good relation, while the slope of attenuation of the reflected slow waves shows a good association with porosity for every thickness. Besides, the reflected wave may affected by scattering effect more compared to the incident wave, thus, cause the correlation between reflected wave parameters with porosity is lower. The overall results suggest, considering fast and slow wave to estimate bone quality might help to improve the measurement accuracy for both techniques.

*Keywords*: Bandlimited deconvolution, fast and slow waves, pulse echo, through transmission, ultrasound



## INTRODUCTION

Cancellous bone supporting propagation of the ultrasound fast and slow wave and previous research found that, various properties of the cancellous bone show relation with parameters of the two modes wave [1-6]. Nevertheless, the anisotropy factor affected the observation of fast and slow wave in time domain and these waves usually overlap with each other and seen as a single wave. [7]. Because of this, several methods to separate fast and slow wave for the through transmissions (TT) technique has been introduced by Wear [8, 9] and one of the methods is bandlimited deconvolution. The bone density estimation based on ultrasound system which employs TT technique can be improved if the analysis of two modes wave was also included. However, the measurement based on TT technique is restricting at certain several parts of the skeletal area, especially at the spine and hip bone since this technique needs two transducers to operate [1, 10]. To solve the problem, pulse echo (PE) technique is proposed as this technique only required single transducer to work and because of that, PE technique has capabilities to measure at the critical bone area. Furthermore, Hosokawa [1, 10-12] performing Finite Difference Time Domain (FDTD) simulation found that, a significant correlation was shown between cancellous bone porosity and reflected fast and slow waves which were measured using PE technique.

Hence, the aim of this paper is to conduct an experiment using TT and PE technique to analyze the correlation of fast and slow wave parameters with various porosities of bone phantom, which is polyurethane (PU) foam. There are three different thicknesses of PU foam involved in this study and the consistency and performance of the correlation coefficient also observed between them. Fast and slow wave will be estimated using a bandlimited deconvolution method from the incident and reflected wave that were obtained using TT and PE measurement technique. After that, the results in terms of the correlation coefficient of the ultrasound parameter will be compared. The comparison will be done between mix, fast and slow waves for both incident and reflected wave for various porosities and thicknesses.

## EXPERIMENTAL

### Materials

The bone phantom chosen for the experiment was Rigid PU foam, Sawbones®. This PU foam has a cell size, microstructure and stress - strain curve equivalent as real human cancellous bone [13]. As shown in Table 1, the porosity level of the PU foam was ranging from 0.73 to 0.9 which divide into five (5) type of PU foam.

**Table 1** Properties of rigid PU foam [14] and water.

| No. | Material and Substance | Φ | Cell size (mm) | Acoustic Impedance (MRayls) | Density (kg/m³) |
|---|---|---|---|---|---|
| 1. | Water | - | - | 1.4 | 1 |
| 2. | PU foam | 0.9<br>0.86<br>0.83<br>0.8<br>0.73 | 0.5 – 2.5<br>0.5 – 2.0<br>0.5 – 1.5<br>0.5 – 1.0<br>0.5 – 1.0 | 1.8 (solid PU) | 1.04 (Solid PU) |

Φ = porosity

Besides, each of the porosity level of PU foam has three different thicknesses (*D*) which are 10 mm, 9 mm, and 8 mm. Although only five samples of PU foam for each thickness, the ranges of the porosity value are sufficient to represent healthy and unhealthy cancellous bone [15].

### Wave measurement technique

Two ultrasound transducers were used for the TT measurement technique, where one transducer employed as a transmitter and another one transducer employed as receiver. On the other hand, only one ultrasound transducer was used for the PE measurement technique and this single transducer will employ as both transmitter and receiver. Moreover, for the PE measurement technique, the aluminum plate was used as a reflector element which acts to reflect the incoming wave back to the transducer. In addition, the range between the transducers with aluminum plate for PE technique and between the two transducers for TT technique was 24 mm and bone phantom (PU foam) was located 12 mm between them as shown in Fig. 1.

The ultrasound transducer (V303-SU, Panametrics Olympus) was a broadband type transducer with 1 MHz of frequency, 13 cm in diameter and 1.5 cm of focal length. A pulser/receiver (5077PR, Panametrics Olympus) was used as a signal generator and capable to operate both for TT and PE measurement technique. 300 Volt peak-to-peak (Vpp) with 25 dB of gain was set to the signal generator. 300 Volt peak-to-peaks ($V_{pp}$) with 25 dB of gain was set to the signal generator. The oscilloscope (Tektronix) was used to receive and digitized the incoming ultrasound signal. Then, the digitized signal was stored in computer via USB (universal serial bus). The analysis software used was Matlab 2015. Moreover, 64 signals are averaged for each measurement taken and measurements are also performed several times.

### Bandlimited Deconvolution Method

Eq.1 represents the numerical models for the propagation of ultrasound wave through the cancellous bone for TT technique. *Y(f)* is the amplitude spectrum of the signal propagate through a sample (mix wave) and *X(f)* is the amplitude spectrum of the signal propagate through a water only (reference wave).

$$Y(f) = X(f)[Hfast(f) + Hslow(f)] \qquad (1)$$

The ultrasound frequency is denoted as *f* and the factor in brackets is represented as a transfer function of fast and slow wave [8, 16]. For the PE technique, the reflected wave, in Fig. 1 (b) (red arrow) is assumed to behave just like through wave or incident wave, thereby, the Eq. 1 can be used to represent propagation of the reflected wave.

Moreover, the principle of Eq. 1 was used by the bandlimited deconvolution method [8, 9]. Briefly, the combination of fast and slow wave transfer function, *Htotal(f)* will be calculated by obtaining the ratio of the fast Fourier transform (FFT) of the wave transmitted through (TT) or reflected and through (PE) PU foam with waves propagate through (TT) or reflected (PE) in water only (reference wave). Then, the *Htotal(f)* is computed into the impulse response, *htotal(t)* by taking the inverse FFT (IFFT). After that, based on a time threshold of local minimum (Hilbert transform envelope) determined by the time shifts corresponding to velocities between 1700 and 1850 m/s which is equivalent to velocities of fast wave, a rectangular time-domain windows will be created. The purpose of the rectangular time-domain window is to separate fast and slow wave impulse responses.

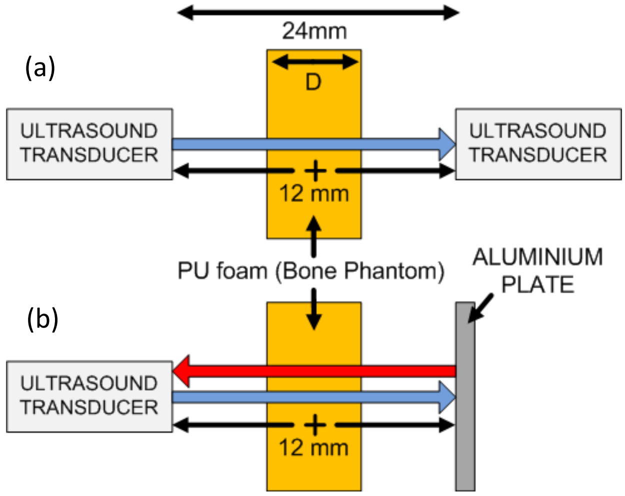


**Fig. 1** Diagram of the ultrasound wave measurement technique for (a) TT and (b) PE. Blue arrow denote as incident wave while red arrow denote as reflected wave.

After that, to obtain a fast wave impulse response, *hfast(t)*, rectangular time-domain window with a value equal to one for the time before the threshold and zero for a time over the threshold will be multiplied with *htotal(t)*. The *hfast(t)* then computed into *Hfast(f)* using FFT and convolved with *X(f)* in order to create a fast wave in frequency domain, *Yfast(f)*. The *Yfast(f)* is computed again using IFFT and become fast wave in time domain, *yfast(t)*. To obtained slow wave in time domain, *yslow(t)*, the mix wave in time domain, *y(t)* subtracted the *yfast(t)*.

### Wave parameter calculation

There are two ultrasound wave parameters involved in this experiment. First one is wave amplitude (*A*) and the other one is frequency dependent attenuation (*β*). To obtain the *A* parameters, the value at the peak magnitude of the wave in frequency domain was observed. The formula for the calculation for the *β* parameters is as follows [8],

$$\beta(f) = \frac{1}{D}\,[20\log SR(f) - 20\log SB(f)] \qquad (2)$$

where *SB(f)* and *SR(f)* is the amplitude spectrum of a sample and reference wave, respectively. The *D* is denoted as the sample thickness in cm. Furthermore, from 0.2 to 0.6 MHz will be the frequency range for the slope *β(f)* and the value is in the unit of dB/cm/MHz.

## RESULTS AND DISCUSSION

### Separation of fast and slow wave

Referring to Fig. 2 (a), the |*h(t)*| is the envelope of the impulse response, *htotal(t)* or *h(t)* for the incident mix wave for the PU foam sample with porosity value of 0.9 and thickness of 9 mm. The impulse response of the fast, *hfast(t)* (left) and slow, *hslow(t)* (right) wave was divided by the time threshold (red dash line). Moreover, based on reference wave adjustment measurement arrival time (i.e., time = 0 µs), the arrival time of incident slow waves was roughly 1.3 µs later than 0 µs. However, the arrival time of incident fast wave cannot be observed in Fig. 2 (a) but can be estimated in Fig. 2 (b) after the transfer function *hfast(t)* was computed into *yfast(t)* (fast wave in time domain). As shown in Figure 2 (b), based on the arrival time of reference wave which was arrived at the time of 18.6 µs, the arrival time of incident fast waves (1.81 µs) was 0.5 µs faster than the reference wave.

The presence of two waves can be seen from the Fig. 2 (a) where the oscillation frequencies were different between *hslow(t)* and *hfast(t)*. The oscillation frequency for *hfast(t)* (0.36 MHz) is lower than *hslow(t)* (0.79 MHz).

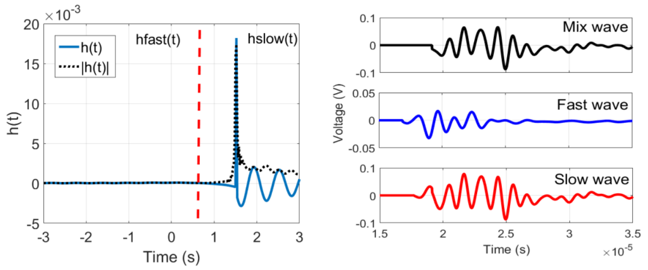


(a) (b)

**Fig. 2** (a) Transfer function and, (b) example of the incident mix, fast and slow wave estimated using bandlimited deconvolution method for the PU foam sample with porosity value of 0.9 and thickness of 9 mm.

Moreover, the low frequency of fast wave also corresponds with the slope of attenuation, where the slope of attenuation of fast wave (53 dB/cm/MHz) was higher than the slow wave (11 dB/cm/MHz). Previous research by Wear [8] also reported the same outcome in terms of frequency differences between fast and slow wave. Still, there are some cases where fast wave has low attenuation and has high amplitude compared to slow wave due to using different material compared to the bone [17, 18]. In this study, the fast wave is assumed to have passed through the solid part of PU foam. Compared to pore part of the PU foam, the solid part has a higher attenuation effect, thereby, the high frequency broadband region of fast wave was attenuated faster and only low frequency region arrived at the receiver. According to previous research [19], high frequency component of ultrasound affected more by attenuation, especially the absorption effect compared to the low frequency component. Due to this phenomenon, fast wave usually has lower frequency and amplitude compared to slow wave.

Fig. 2 (b) demonstrated the incident mix wave, *ytotal(t)*, as well as fast, *yfast(t)* and slow, *yslow(t)* wave that were estimated using a bandlimited deconvolution method for PU foam sample with a porosity value of 0.9 and thickness of 9 mm. The observation in Fig. 2 (b) shows that, the mix wave's $V_{pp}$ was 0.10 V. Moreover, the fast wave's $V_{pp}$ (0.048 V) was lower than slow wave's $V_{pp}$ (0.070 V). The same findings also reported by previous researches in the investigation with bone phantom and real bone [1-6] in terms of ratio of fast and slow wave amplitude.

## Waves parameters versus various porosities

Referring to Table 2 – TT (Incident wave), wave amplitudes for all incident wave ($A_I$) decrease when porosity increase and shows a clear correlation except at the thickness of 8 mm, where the correlation coefficient for both $A_{Imix}$ and $A_{Islow}$ was slightly lower. The $\beta_{Ifast}$ shows a positive trend with a good correlation against porosity but the correlation coefficient was slightly lower at the thickness of 9 mm. The $\beta_{Imix}$ and $\beta_{Islow}$ shows a negative trend and low correlation versus porosity except at the thickness of 8 mm where the correlation coefficient both waves demonstrate a moderately relevant association with porosity.

Referring to Table 2 – PE (Reflected wave), only $A_{Rslow}$ and $A_{Rmix}$ shows a significant correlation coefficient at the thickness of 10 mm for the amplitude parameters. However, both parameters demonstrated low correlation at the thickness 9 and 8 mm. In terms of slope of attenuation, the $\beta_{Rslow}$ shows a negative trend versus porosity with a good correlation coefficient at the thickness of 9 mm and 8 mm, but slightly lower at the thickness of 10 mm. In addition, $\beta_{Rfast}$ displays positive trend versus porosity and overall correlation coefficient were slightly significant except at the thickness of 10 mm. However, $\beta_{Rmix}$ shows no significant relationship with porosity for each thickness.

The negative trends of the amplitude of the incident waves versus porosity indicate the high attenuation effect, especially scattering when pore size and the degree of inhomogeneity of porous structure increase [19-21]. Conversely, for the real bone application, higher density contributes to higher attenuation [22, 23]. The real bone has the acoustic impedance value of 7.5 MRayls and typical density value of 2000 kg/m$^3$ [24], which is very different compare to water or bone marrow. Due to the impedance differences between water and bone, the high scattering effect also occurs at the low porosity of bone [19]. Hence, the effect similar to the bone sonometry takes place, where decreases of porosity cause increase of attenuation effect [25]. Compared to PU foam, its acoustic impedance and density almost the same with water (refer tables 1), thus, the absorption dominates the attenuation effect at the low porosity.

As porosity increases, the effects of scattering also increase due to increase the degree of inhomogeneity. This may indicate that, the effect of scattering due to acoustic impedance mismatch is higher compared to inhomogeneity of trabecular structure. In addition, the increases trends of $\beta_{Imix}$ does not parallel with the decreases $A_{Imix}$ versus porosity. This might be due to overlapping of two waves causing the $\beta_{Imix}$ not show its true manners. For the reflected wave amplitude ($A_R$), the wave may be weakened as it has been reflected and absorbed on the surface of the aluminum plate. The wave also propagate through the PU foam twice as much and may be mix with the wave scattered inside (generated during propagation of incident wave) the porous structure of the PU foam and affect the relation of all reflected wave amplitude against porosity.

Additionally, the decreasing trend of all incident wave amplitude versus porosity is just like the fast wave [4, 7, 25]. The fast wave is the wave that spreads through the solid portion of the overall porous structure [7]. Unlike the incident mix waves, the decreases of $A_{Ifast}$ correspond with increases of $\beta_{Ifast}$ versus porosity. Other researcher also found that, speed and amplitude of fast wave increase with bone density while the opposite happen to the slow wave [4]. Cardoso *et al.* [5] investigating using real bone indicates that, the slope of attenuation of fast wave demonstrated a negative parabolic curve response versus porosity. For the most porous cancellous bone samples, the slow wave was the most dominance and has concealed the slope of attenuation value of fast wave. Because of that, slope of attenuation value of fast wave was force to decrease until reach the same value as the slope of attenuation of the slow wave as the porosity increase [5]. Contrariwise, Hoffman *et al.* [25] which investigate real bone and utilizing the Bayesian method to separates fast and slow wave from mix wave shows that, slope of attenuation value for both fast and slow wave presenting negative trends versus porosity and the phenomenon is known as bone sonometry.

**Table 2** Correlation coefficient of wave parameters versus various porosities for TT and PE technique.

| Type of wave | Wave Parameters | *D* (mm) | Correlation Coefficient, $R^2$ | | |
|---|---|---|---|---|---|
| | | | Mix wave | Fast wave | Slow wave |
| TT (Incident wave) | Amplitude ($A_I$) | 10 | -0.88 ($p <$ 0.05) | -0.88 ($p <$ 0.05) | -0.86 ($p <$ 0.05) |
| | | 9 | -0.90 ($p <$ 0.05) | -0.70 ($p <$ 0.1) | -0.88 ($p <$ 0.05) |
| | | 8 | -0.67 ($p <$ 0.1) | -0.74 ($p <$ 0.1) | -0.60 ($p <$ 0.1) |
| | Frequency Dependent Attenuation ($\beta_I$) | 10 | -0.25 ($p >$ 0.1) | 0.88 ($p <$ 0.05) | -0.22 ($p >$ 0.1) |
| | | 9 | -0.28 ($p >$ 0.1) | 0.68 ($p <$ 0.1) | -0.28 ($p >$ 0.1) |
| | | 8 | -0.57 ($p =$ 0.1) | 0.84 ($p <$ 0.05) | -0.73 ($p =$ 0.05) |
| PE (Reflected wave) | Amplitude ($A_R$) | 10 | -0.75 ($p =$ 0.05) | -0.27 ($p >$ 0.1) | 0.61 ($p <$ 0.1) |
| | | 9 | 0.0007 ($p$ $>$ 0.1) | -0.06 ($p >$ 0.1) | 0.11 ($p >$ 0.1) |
| | | 8 | 0.10 ($p >$ 0.1) | 0.22 ($p >$ 0.1) | 0.04 ($p >$ 0.1) |
| | Frequency Dependent Attenuation ($\beta_R$) | 10 | -0.001 ($p$ $>$ 0.1) | 0.45 ($p >$ 0.1) | -0.63 ($p <$ 0.1) |
| | | 9 | 0.21 ($p >$ 0.1) | 0.63 ($p <$ 0.1) | -0.82 ($p <$ 0.05) |
| | | 8 | 0.10 ($p >$ 0.1) | 0.51 ($p <$ 0.1) | -0.76 ($p =$ 0.05) |

Sign (±) indicate positive or negative trend versus porosity
n = 5, P > 0.1 = not significant, 0.05 < p ≤ 0.1 = slightly significant, 0.01 < p ≤ 0.05 = significant, p ≤ 0.01 = highly significant.

Nevertheless, in this study, $\beta_{Ifast}$ shows a positive trend versus porosity. Since the fast wave transmit mainly through the solid region of the porous structure, the absence of solid formation (increase porosity) give rise to the attenuation effect, especially scattering at the most porous of the PU foam. Compared with the result obtained by Hoffman *et al*. [25], the density and acoustic impedance of PU does not contribute much to the attenuation because the value for both parameters are almost the same with water (refer to Table 1). In terms of the reflected fast wave, the $\beta_{Rfast}$ shows the same consistent trends with $\beta_{Ifast}$ but slightly lower relation with porosity for every thickness.

The result also shows that, $\beta_{Islow}$ demonstrate a trend parallel with previous research where the slope of attenuation decrease when porosity increase [25]. However, another researcher [5] described that, the slope of attenuation of slow wave rise when porosity increases. For the $\beta_{Islow}$, When the porosity and the trabecular arrangement getting farther with each other, both cell and pore size of the cellular PU foam also increase, thus enhance the fluid motion and at the same time, decrease the resistance of ultrasound propagation. This occurrence will result in decreases of the attenuation effect of the slow wave [26]. The explanations also supported the claim that slow waves propagate mainly through pore part of the porous structure [7]. Moreover, the $\beta_{Rslow}$ shows a good correlation with porosity for every thickness compared to the $\beta_{Islow}$. The attenuation effect, especially scattering due to propagation path of reflected wave (as mentioned previously) may affect the reflected fast wave since this wave passing through the solid portion of the overall area of the porous structure. Because of that, overall reflected wave parameters were dominated by slow wave. Meanwhile, the fast wave may possibly dominate the propagation of the incident wave and causing the correlation coefficient of $\beta_{Islow}$ to be lower compared to $\beta_{Rslow}$. As investigated by Hosokawa [1, 10, 12], fast and slow wave can also exist in backscattered wave. Based on the findings, it can be assumed that the reflected fast and slow wave arrives at the transducer and captured during analysis may not "perfect" because some of the waves propagate with backscattered waves. This is also possibly the reason why overall correlation coefficient parameters reflected wave with porosity lower compared to the incident wave.

Furthermore, the performance of the correlation coefficient for all parameters both incident and reflected waves seems affected by the thickness. For instance, the correlation coefficient of $\beta_{Islow}$ increase when the thickness decrease. The decreases of thickness reduce the solid part of the PU foam and may reduce the domination of fast wave, hence, provide a good correlation coefficient for incident slow wave. The fast wave required certain thickness of solid trabeculae in order to propagate [27]. However, the number of thicknesses used maybe not sufficed to observe the effect of thickness toward ultrasound waves. Hence, increasing the number of thicknesses (add more thickness from 10 mm to 5 mm) might help to perceive the influence of thickness with ultrasound waves.

The limitation in this study is the small number of samples which is five (5) samples for each thickness. Because of that, the result affecting the significant level (p-value) required correlation coefficient to achieve at least 0.8 for the p-value to reach below 0.05. In this paper, slightly significant ($0.05 < p \leq 0.1$) also considered as slightly good correlation coefficient ($R^2 = 0.45$). Another limitation is the material used has dissimilar acoustic characteristics compared to real cancellous bones.

## CONCLUSION

In conclusion, both incident and perhaps reflected wave can be separated into individual fast and slow wave using bandlimited deconvolution method. The slope of attenuation of the incident fast wave shows a consistent positive trend and clear correlation versus porosity compared to other parameters for every thickness. Meanwhile, the slope of attenuation of the reflected slow wave shows a consistent negative fashions and good relation against porosity for every thickness. However, the incident slow and reflected fast waves also show a consistent trend versus porosity despite lower correlation coefficient. It shows that, the fast and slow wave sensitive with the microstructure of PU foam compared to mix wave despite the material used is different compared to the bone. The thickness also seems affected some of the wave parameters. In addition, reflected wave may be affected by the attenuation effect more than incident wave and resulting in low correlation coefficient for the reflected wave, especially fast wave with porosity. Overall result propose that, take into account of fast and slow wave to predict bone health based on ultrasound might help to improve the quantification precision for both TT and PE technique.

## ACKNOWLEDGEMENT

This work was financially supported by the Universiti Teknologi Malaysia under the Research University Grant Q.J130000.2551.21H49.

## REFERENCES

[1] Hosokawa, A. (2015). Numerical analysis of ultrasound backscattered waves in cancellous bone using a finite-difference time-domain method: isolation of the backscattered waves from various ranges of bone depths. *IEEE Transactions on Ultrasonics, Ferroelectrics, And Frequency Control*, *62*(6), 1201-1210.

[2] Nagatani, Y., Nguyen, V. H., Naili, S., Haïat, G. (2015). The effect of viscoelastic absorption on the fast and slow wave modes in cancellous bone. *6th European Symposium on Ultrasonic Characterization of Bone* (pp. 1-2).

[3] Kawasaki, S., Ueda, R., Hasegawa, A., Fujita, A., Mihata, T., Matsukawa, M., Neo, M. (2015). Ultrasonic wave properties of human bone marrow in the femur and tibia. *The Journal of the Acoustical Society of America*, *138*(1), EL83-EL87

[4] Otani, T. (2005). Quantitative estimation of bone density and bone quality using acoustic parameters of cancellous bone for fast and slow waves. *Japanese journal of applied physics*, *44*(6S), 4578.

[5] Cardoso, L., Teboul, F., Sedel, L., Oddou, C., Meunier, A. (2003). In vitro acoustic waves propagation in human and bovine cancellous bone. *Journal of Bone and Mineral Research*, *18*(10), 1803-1812.

[6] Nelson, A. M., Hoffman, J. J., Holland, M. R., Miller, J. G. (2012, October). Single mode analysis appears to overestimate the attenuation of human calcaneal bone based on Bayesian-derived fast and slow wave mode analysis. *IEEE International Ultrasonics Symposium* (pp. 1015-1018).

[7] Hosokawa, A., Nagatani, Y., Matsukawa, M. (2011). The fast and slow wave propagation in cancellous bone: Experiments and simulations. In *Bone Quantitative Ultrasound* (pp. 291-318). Springer.

[8] Wear, K. A. (2014). Time-domain separation of interfering waves in cancellous bone using bandlimited deconvolution: Simulation and phantom study. *The Journal of the Acoustical Society of America*, *135*(4), 2102-2112.

[9] Wear, K., Nagatani, Y., Mizuno, K., Matsukawa, M. (2014). Fast and slow wave detection in bovine cancellous bone in vitro using bandlimited deconvolution and Prony's method. *The Journal of the Acoustical Society of America*, *136*(4), 2015-2024.

[10] Hosokawa, A. (2015, October). Numerical analysis of fast and slow waves backscattered from various depths in cancellous bone. *IEEE International Ultrasonics Symposium (IUS)* (pp. 1-4).

[11] Hosokawa, A. (2013, July). Variations in reflection properties of fast and slow longitudinal waves in cancellous bone with boundary condition. *IEEE International Ultrasonics Symposium (IUS)* (pp. 2076-2079).

[12] Hosokawa, A. (2014). Numerical investigation of reflection properties of fast and slow longitudinal waves in cancellous bone: Variations with boundary medium. *Japanese Journal of Applied Physics*, *53*(7S), 07KF13.

[13] Shim, V., Boheme, J., Josten, C., Anderson, I. (2012). Use of polyurethane foam in orthopaedic biomechanical experimentation and simulation. *Polyurethane*, 171-200.

[14] S. Worldwide. Biomechanical Test Materials Catalogue. *Vashon, WA*.

[15] Laugier, P., Haïat, G. (Eds.). (2011). *Bone quantitative ultrasound* (Vol. 576). Springer.

[16] Marutyan, K. R., Holland, M. R., Miller, J. G. (2006). Anomalous negative dispersion in bone can result from the interference of fast and slow waves. *The Journal of the Acoustical Society of America*, *120*(5), EL55-EL61.

[17] Anderson, C. C., Bauer, A. Q., Holland, M. R., Pakula, M., Laugier, P., Bretthorst, G. L., Miller, J. G. (2010). Inverse problems in cancellous

bone: Estimation of the ultrasonic properties of fast and slow waves using Bayesian probability theory. *The Journal of the Acoustical Society of America*, *128*(5), 2940-2948.

[18] Anderson, C. C., Bauer, A. Q., Marutyan, K. R., Holland, M. R., Pakula, M., Bretthorst, G. L., ... & Miller, J. G. (2011). Phase velocity of cancellous bone: Negative dispersion arising from fast and slow waves, interference, diffraction, and phase cancellation at piezoelectric receiving elements. In *Bone Quantitative Ultrasound* (pp. 319-330). Springer.

[19] Wear, K. A. (2008). Ultrasonic scattering from cancellous bone: a review. *IEEE Transactions on Ultrasonics, Ferroelectrics, and Frequency Control*, *55*(7), 1432-1441.

[20] F Padilla, F., Wear, K. (2011). Scattering by trabecular bone. In *Bone Quantitative Ultrasound* (pp. 123-145). Springer.

[21] Pakula, M. (2015, June). On the modeling of wave propagation in cancellous bone. *6th European Symposium on Ultrasonic Characterization of Bone* (pp. 1-4).

[22] Gilbert, R. P., Guyenne, P., Li, J. (2013). A viscoelastic model for random ultrasound propagation in cancellous bone. *Computers & Mathematics with Applications*, *66*(6), 943-964.

[23] Nelson, A. M., Hoffman, J. J., Anderson, C. C., Holland, M. R., Nagatani, Y., Mizuno, K., ... & Miller, J. G. (2011). Determining attenuation properties of interfering fast and slow ultrasonic waves in cancellous bone. *The Journal of the Acoustical Society of America*, *130*(4), 2233-2240.

[24] Litniewski, J. (2005). Determination of the elasticity coefficient for a single trabecula of a cancellous bone: Scanning Acoustic Microscopy approach. *Ultrasound in Medicine & Biology*, *31*(10), 1361-1366.

[25] Hoffman, J. J., Nelson, A. M., Holland, M. R., Miller, J. G. (2012). Cancellous bone fast and slow waves obtained with Bayesian probability theory correlate with porosity from computed tomography. *The Journal of the Acoustical Society of America*, *132*(3), 1830-1837.

[26] Lee, K. I. (2016). Relationships of linear and nonlinear ultrasound parameters with porosity and trabecular spacing in trabecular-bone-mimicking phantoms. *The Journal of the Acoustical Society of America*, *140*(6), EL528-EL533.

[27] Nagatani, Y., Mizuno, K., Saeki, T., Matsukawa, M., Sakaguchi, T., Hosoi, H. (2008). Numerical and experimental study on the wave attenuation in bone–FDTD simulation of ultrasound propagation in cancellous bone. *Ultrasonics*, *48*(6-7), 607-612.